

# ANOTHER TURBO-SOMETHING : CARRIER SYNCHRONIZATION

*Luca Giugno, Vincenzo Lottici, Marco Luise*

University of Pisa — Dipartimento Ingegneria Informazione

Via Diotisalvi, 2 — I-56122 Pisa, Italy

Tel. +39 050 568511 — Fax +39 050 569522 - e-mail: v.lottici@iet.unipi.it

## ABSTRACT

We introduce in this paper a low-complexity joint carrier frequency and phase recovery algorithm for coherent detection/decoding of a turbo-coded 16-QAM signal. The estimator (which can be actually applied to any linear modulation scheme) is based on a pseudo-Maximum Likelihood (ML) approach, and unlike previously published works, makes *iterative* use of soft decisions provided by the SISO (Soft-In Soft-Out) decoders within the overall iterative turbo decoding scheme, yielding negligible degradation with respect to ideal carrier synchronization. Performance in terms of mean estimated value, mean-squared estimation error, and overall decoder Bit Error Rate (BER) as derived by simulation are also reported.

## 1. INTRODUCTION

The impressive performance of turbo codes has triggered in the last decade a lot of research addressing the application of this powerful coding technique in digital wireless communications [1]-[3]. When applied to linear modulations, in order to reach a performance which is close to Shannon capacity on the AWGN channel, one has to implicitly assume ideal coherent detection, or, in other words, the carrier reference has to be estimated before the data can be decoded. Therefore, the problem is how to achieve a fast and accurate carrier synchronization (due to the instability of the oscillators and the Doppler effect) from the received signal at those extremely low signal-to-noise ratios typical of such codes.

In the technical literature, a great effort is being devoted to the development of carrier recovery techniques for demodulation of coded signals [4]-[8]. Reference [4] gives a good example of a low-complexity algorithm, but does not take into account the code structure. In [5] the tentative decisions of the first SISO decoder, which is based on a Soft Output Viterbi Algorithm, are used in the phase recovery system. The estimation method proposed in [6] uses soft decisions in the form of a posteriori probabilities at each iteration of the Expectation-Maximization (EM) algorithm but is mainly developed for uncoded signals. Two main works have appeared in the literature [7]-

[8], based on a soft-output adaptive receiver. They both consist of forward and backward recursions (based on add-compare-select steps) operating on a trellis where the unknown phase is estimated by some sort of per-survivor parameter estimation.

The aim of this paper is to introduce a low-complexity joint carrier phase and frequency recovery technique suited for turbo coded QAM receivers. Our algorithm is suggested by a Maximum Likelihood (ML) carrier synchronization approach, and makes *iterative* use of soft decisions provided by the SISO constituent decoders at each iteration. Therefore, iterative decoding and carrier recovery go together iteration after iteration in a sort of *iterative soft decision directed* (ISSD) mode. This allows to perform reliable carrier estimation and almost ideal coherent detection for values of the Signal-to-noise Ratio (SNR) down to a few dB only, and without the need to resort to narrowband phase-locked loops (PLL) with large acquisition time.

## 2. SYSTEM MODEL

The baseband-equivalent model of a turbo coded transmission system is depicted in Fig. 1a. The binary information data bits are grouped into blocks of  $Q$  bits each, that are fed into the rate- $r$  turbo encoder shown in Fig. 1b [3] consisting of two identical RSC codes with parallel concatenation via random interleaving. The feedback and the feedforward sections of the RSC encoders are described by the primitive polynomials  $g_2$  and  $g_1$ , respectively. The parity (redundant) bits out of the two encoders are properly punctured to reduce coding overhead, and to achieve the desired overall rate,  $r$ . The resulting block of  $Q/r$  systematic (information) plus parity (redundancy) data bits are then Gray-mapped onto a QAM constellation, whose symbols are transmitted over an AWGN channel with two-sided power spectral density  $N_0/2$ .

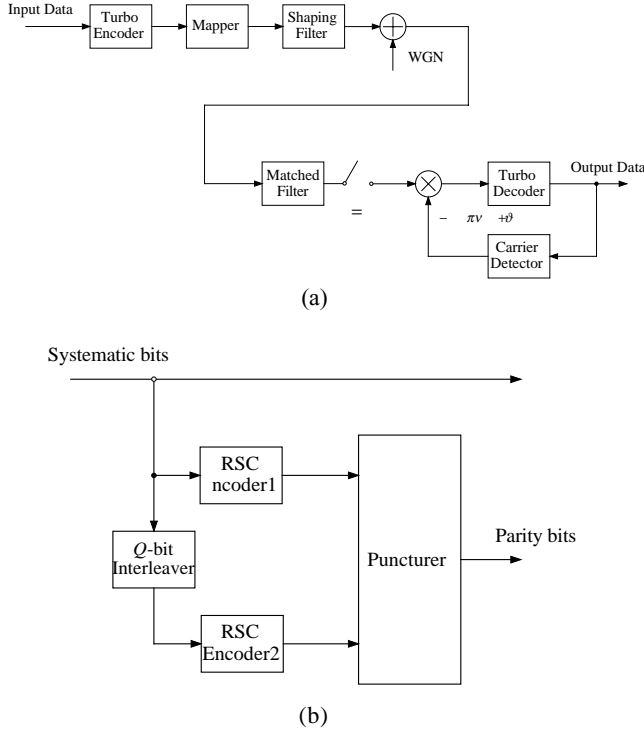


Fig. 1 – Turbo-coded transmission system (a) and Turbo-encoder (b) schematic.

Assuming that gain control, symbol timing recovery, and code frame synchronization are properly carried out, and intersymbol interference is negligible, the symbol-rate output of the receiver matched filter is

$$x[m] = c_m e^{j(2\pi\nu mT + \vartheta)} + w[m] \quad (1)$$

where  $c_m$  is a unit-energy QAM symbol,  $w[m]$  is a complex-valued zero-mean Gaussian noise sample with independent components, each with variance  $N_0/(2E_s)$ , ( $E_s/N_0$  is the ratio between the received energy-per-symbol and the one-sided noise power spectral density), and finally  $\vartheta$  and  $\nu$  are the unknown carrier phase and frequency offsets to be estimated, respectively.

The iterative decoding procedure is based on a modified version of the BCJR algorithm [1] for symbol-by-symbol Maximum-A-posteriori Probability (MAP) detection. At the first iteration step, the matched filter output  $x[m]$  is used by the first BCJR decoder (DEC1) to compute the so-called *log a posteriori probability ratio* (LAPPR) for the generic  $n$ -th information bit  $u_n$  in the data block under decoding, given as follows

$$L(u_n) = \log \left( \frac{\Pr\{u_n = 1 | \mathbf{x}\}}{\Pr\{u_n = -1 | \mathbf{x}\}} \right) \quad (2)$$

where  $\mathbf{x}$  is the vector of the matched filter output samples within a code block. With their sign, the LAPPRs allow to take MAP decisions on each transmitted bit. Also,

their absolute values represent a sort of *reliability* metric about the estimated value of each bit: the more the LAPPR is large (in absolute value), the more the two probabilities are unbalanced, and the more reliable the hard decision is (with high probability). The LAPPRs are used as *soft* inputs (i.e., continuous-amplitude samples) to the second BCJR decoder (DEC2) to perform the next iteration step. The output of DEC2 is in turn fed back to DEC1 as an additional soft input (the so-called *extrinsic information*) to compute new, updated values of  $L(u_n)$ , and the iteration goes on this way, until a steady-state is reached after some iterations. Decoding is stopped, and the hard-decisions on the latest values of  $L(u_n)$  are output.

In the next Section, we will derive a joint carrier phase and frequency offset estimation algorithm based on those LAPPR values, that we can label iterative soft-decision directed (ISDD). Such estimator works in tandem with the iterative decoding, takes advantage of the progressive reliability improvement inherent in iterative decoding, and eventually comes to a improved carrier estimate at the end of the iterative process.

### 3. SOFT-DECISION-DIRECTED CARRIER PHASE AND FREQUENCY ESTIMATION

#### 3.1. Joint phase and frequency estimation

Assuming that  $\mathbf{x} \triangleq [x[0], x[1], \dots, x[N-1]]^T$  is the vector of signal samples taken at the output of the receiver matched filter within a single  $Q$ -bit code block ( $N = Q/(4r)$  for 16-QAM), and neglecting irrelevant multiplicative factors, the likelihood function (LF) for the estimation of  $\vartheta$  and  $\nu$  based on the observation of such a block is [9]

$$\Lambda(\mathbf{x}|\tilde{\nu}, \tilde{\vartheta}, \tilde{\mathbf{c}}) = \exp \left\{ \frac{1}{N_0} \operatorname{Re} \left\{ \sum_{m=0}^{N-1} x[m] \tilde{s}^*[m] \right\} - \frac{1}{2N_0} \sum_{m=0}^{N-1} |\tilde{s}[m]|^2 \right\} \quad (3)$$

where  $\tilde{s}[m]$  is defined as

$$\tilde{s}[m] \triangleq \tilde{c}_m e^{j(2\pi\tilde{\nu}mT + \tilde{\vartheta})} \quad (4)$$

and  $\tilde{\mathbf{c}} \triangleq [\tilde{c}_0, \tilde{c}_1, \dots, \tilde{c}_{N-1}]^T$ ,  $\tilde{\nu}$ ,  $\tilde{\vartheta}$  are *trial* values of the symbol sequence, the carrier frequency offset, and the carrier phase, respectively. Considering  $\tilde{\mathbf{c}}$  as a *nuisance parameter*, the ML estimates for the frequency  $\nu$  and phase  $\vartheta$  are given by

$$(\hat{\nu}, \hat{\vartheta}) = \arg \max_{\tilde{\nu}, \tilde{\vartheta}} \left\{ \Lambda(\mathbf{x}|\tilde{\nu}, \tilde{\vartheta}) \right\} \quad (5)$$

where the marginal likelihood function

$$\Lambda(\mathbf{x}|\tilde{\nu}, \tilde{\vartheta}) \triangleq E_{\tilde{\mathbf{c}}} \left\{ \Lambda(\mathbf{x}|\tilde{\nu}, \tilde{\vartheta}, \tilde{\mathbf{c}}) \right\} \quad (6)$$

is obtained by averaging  $\Lambda(\mathbf{x}|\tilde{\nu}, \tilde{\vartheta})$  over all of the modulation symbols in a block. Substituting (4) into (3), and assuming, as a first approximation, that  $\{c_m\}$  is a sequence of i.i.d. symbols, averaging over  $\tilde{\mathbf{c}}$  gives

$$\Lambda(\mathbf{x}|\tilde{\nu}, \tilde{\vartheta}) = \prod_{m=0}^{N-1} \sum_{n=0}^{L-1} P_n^{(m)} \exp \left\{ \frac{1}{N_0} \operatorname{Re} \left\{ x(m) C_n^* e^{j(2\pi\tilde{\nu}mT + \tilde{\vartheta})} \right\} \right\} \quad (7)$$

Such an approximation avoids knowledge of the joint statistics of  $\tilde{\mathbf{c}}$  (which is not as easy to derive since those symbols result from the operation of coding and mapping) and is partially motivated by both *systematic* arrangement of the encoder and by possible channel interleaving at the output of the encoder, which contribute to randomize the transmitted symbols. In (7),  $L=16$  is the number of points in the 16-QAM constellation, and  $C_n$  is the generic such element, with an arbitrary ordering. Therefore, using the *a posteriori* probabilities  $P_n^{(m)} \triangleq \Pr\{\tilde{c}_m = C_n | \mathbf{x}\}$  (that we assume here to be known) for the computation of the expectation over the symbols  $\tilde{\mathbf{c}}$ , a low SNR approximation of the pseudo-log-likelihood function (obtained expanding the exp and the log functions into a power series up to the linear term only) turns out to be

$$\lambda(\mathbf{x}|\tilde{\nu}, \tilde{\vartheta}) = \operatorname{Re} \left\{ \sum_{m=0}^{N-1} x(m) \alpha_m^* e^{j(2\pi\tilde{\nu}mT + \tilde{\vartheta})} \right\} \quad (8)$$

where the complex-valued coefficients  $\alpha_m$  are

$$\alpha_m \triangleq \sum_{n=0}^{L-1} P_n^{(m)} C_n \quad (9)$$

Finally, eq. (8) can be easily maximized as a function of  $\tilde{\nu}$  and  $\tilde{\vartheta}$  as follows

$$\begin{cases} \hat{\nu} = \arg \max_{\tilde{\nu}} \{ |X(\tilde{\nu})| \} \\ \hat{\vartheta} = \arg \{ X(\tilde{\nu})|_{\tilde{\nu}=\hat{\nu}} \} \end{cases} \quad (10)$$

where

$$X(\tilde{\nu}) \triangleq \sum_{m=0}^{N-1} x(m) \alpha_m^* e^{-j2\pi\tilde{\nu}mT} \quad (11)$$

### 3.2. Iterative Soft-Decision-Directed phase and frequency estimation

To make our estimation algorithm given by (10) works together with turbo iterative decoding, we observe that the generic constellation point  $C_n$  is associated with a particular 4-bit pattern provided by the encoder. Let us denote with  $[a_1^{(m)}, a_2^{(m)}, b_1^{(m)}, b_2^{(m)}]$  the four (encoded) bits mapped onto the  $m$ -th 16-QAM symbol, where  $a_1^{(m)}, b_1^{(m)}$  identify the *quadrant* of the complex plane wherein  $c_m$  lies (most protected bits), while  $a_2^{(m)}, b_2^{(m)}$  further characterize the position of the symbol within the 4 sub-

constellations in each quadrant (less protected bits). Let us also define

$$P_{a_1}^{(m)} \triangleq \Pr\{a_1^{(m)} = 1 | \mathbf{x}\} \quad (12a)$$

$$P_{a_2}^{(m)} \triangleq \Pr\{a_2^{(m)} = 1 | \mathbf{x}\} \quad (12b)$$

$$P_{b_1}^{(m)} \triangleq \Pr\{b_1^{(m)} = 1 | \mathbf{x}\} \quad (12c)$$

$$P_{b_2}^{(m)} \triangleq \Pr\{b_2^{(m)} = 1 | \mathbf{x}\} \quad (12d)$$

The LAPPR for bit  $a_1^{(m)}$  at the  $l$ -th decoding iteration is given by

$$L_l(a_1^{(m)}) = \log \left( \frac{\Pr\{a_1^{(m)} = 1 | \mathbf{x}\}}{\Pr\{a_1^{(m)} = -1 | \mathbf{x}\}} \right) = \log \left( \frac{P_{a_1}^{(m)}(l)}{1 - P_{a_1}^{(m)}(l)} \right) \quad (13)$$

and similar equations hold for  $P_{a_2}^{(m)}(l)$ ,  $P_{b_1}^{(m)}(l)$ ,  $P_{b_2}^{(m)}(l)$  as functions of the respective LAPPRs  $L_l(a_2^{(m)})$ ,  $L_l(b_1^{(m)})$ ,  $L_l(b_2^{(m)})$ . Under the further assumption that the four bits  $[a_1^{(m)}, a_2^{(m)}, b_1^{(m)}, b_2^{(m)}]$  are independent, after some algebra we find [10]

$$\begin{aligned} \alpha_m^{(l)} = & \tanh \frac{L_l(a_1^{(m)})}{2} \left[ 2 + \tanh \frac{L_l(a_2^{(m)})}{2} \right] + \\ & + j \tanh \frac{L_l(b_1^{(m)})}{2} \left[ 2 + \tanh \frac{L_l(b_2^{(m)})}{2} \right] \end{aligned} \quad (14)$$

that, together with (10) and (14), gives us the chance of devising an iterative estimator as follows:

At iteration #  $l=0$ , start with  $\hat{\nu}_0 = 0$  and  $\hat{\vartheta}_0 = 0$  and

let  $y_0[m] \triangleq x[m]$ ; then, at iteration # $l$ ,  $1 \leq l \leq M-1$ :

- i) Perform soft decision (14) on all symbols  $c_m$  in a given data block ( $0 \leq m \leq N-1$ );
- ii) Compute the  $l$ -th frequency offset estimate  $\hat{\nu}_l$  according to

$$\hat{\nu}_l = \arg \max_{\tilde{\nu}} \left\{ \left| \sum_{m=0}^{N-1} x(m) \alpha_m^{*(l)} e^{-j2\pi\tilde{\nu}mT} \right| \right\} \quad (15)$$

- iii) Compute the  $l$ -th phase estimate  $\hat{\vartheta}_l$  according to

$$\hat{\vartheta}_l = \arg \left\{ \sum_{m=0}^{N-1} x(m) \alpha_m^{*(l)} e^{-j2\pi\hat{\nu}_l mT} \right\}_{\tilde{\nu}=\hat{\nu}_l} \quad (16)$$

- iv) Pre-frequency/phase correct the matched filter output for the next decoding/estimation iteration, according to  $y_l[m] \triangleq x[m] e^{-j2\pi\hat{\nu}_l mT + \hat{\vartheta}_l}$ .

This kind of algorithm, as already mentioned, can be labeled as *Iterative Soft-Decision Directed* (ISDD), since frequency/phase estimation is performed iteratively within each code block by exploiting the *soft decisions* provided by the decoder.

If the reliability for the  $m$ -th symbol at the  $l$ -th iteration is small, i.e., if we jointly have  $L_l(a_1^{(m)}) \approx 0$ ,  $L_l(a_2^{(m)}) \approx 0$ ,  $L_l(b_1^{(m)}) \approx 0$ ,  $L_l(b_2^{(m)}) \approx 0$ , the contribution of such a symbols to (15)-(16) is negligible, contrarily to what happens with conventional decision directed estimation. On the contrary, if the reliability for the  $m$ -th symbol at  $l$ -th iteration is large, i.e., if we have  $|L_l(a_1^{(m)})| \gg 1$ ,  $|L_l(a_2^{(m)})| \gg 1$ ,  $|L_l(b_1^{(m)})| \gg 1$ ,  $|L_l(b_2^{(m)})| \gg 1$ , we get

$$\alpha_m^{(l)} \approx \text{sign}[L_l(a_1^{(m)})] \cdot [2 + \text{sign}[L_l(a_2^{(m)})]] + j \text{sign}[L_l(b_1^{(m)})] \cdot [2 + \text{sign}[L_l(b_2^{(m)})]] \quad (17)$$

and our soft decision boils down to a conventional multi-level hard decisions.

#### 4. SIMULATION RESULTS

Our simulations were carried out with a  $r = 3/4$  turbo encoder based on the parallel concatenation of two identical binary 16-state rate-1/2 RSC encoders with generators  $g_1 = (31)_8$  and  $g_2 = (33)_8$ , via a pseudo-random interleaver with block length  $Q = 1500$ , and using 16-QAM as modulation format. In the following, the performance of the estimation algorithm will be assessed through numerical evaluation of the mean estimated value (MEV), the root-mean squared estimation error (RMSEE) and the overall BER performance of the coded system with joint phase and frequency recovery taking the number of the decoder iterations  $M$  and the energy per bit to noise spectral density ratio  $E_b/N_0$  as the main design parameters. As far as the calculation of the frequency offset given by (15) is concerned, we used a zero-padded FFT algorithm with  $N_{FFT}$  points ( $N_{FFT} > 500$ ). The coarse maximum search over all FFT bins is also refined by a subsequent stage of local parabolic interpolation around the coarse maximum.

##### 4.1. MEV curves

Figure 2 depicts the phase MEV curves of the ISDD phase estimation algorithm (i.e., the average estimated value  $E\{\hat{\vartheta}\}$  as a function of the true phase offset  $\vartheta$ ) for different numbers of decoder iterations  $M = 6, 8, 10, 12$ , with  $E_b/N_0 = 6$  dB and with ideal frequency offset estimation. This value of the signal-to-noise ratio roughly corresponds to a BER of about  $10^{-5}$  with ideal phase recovery. The usual  $\pi/2$  estimation ambiguity due to the rotational symmetry of the QAM constellation is apparent, even if this was not obvious in advance, since rotational symmetry may be in general destroyed by the use of a channel encoder. The information data can be recovered, provided that the residual ambiguity is resolved by the same means as with uncoded transmission (unique word, differential encoding, etc.). The difference between the MEV curves is

not significant for phase errors  $|\vartheta| \leq 20^\circ$ , whatever the number of iterations, whereas with larger phase errors the bias of the algorithm is negligible only for  $M = 10, 12$ .

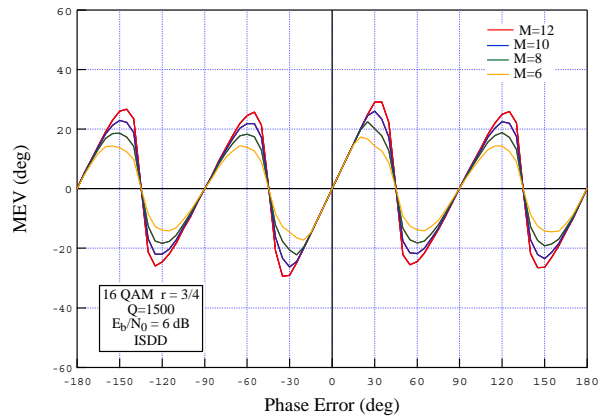


Fig. 2 — Phase Mean Estimated Value (MEV) curves with different iteration numbers (ideal frequency recovery).

The MEV curves illustrated above show strong bias in the vicinity of  $\pm\pi/4$  and multiples, suggesting to use this estimator as a sort of phase error detector in a time-recursive recovery scheme. This has been done on a block-by-block basis as follows: the estimate obtained in the  $m$ -th code block is used to pre-correct all of the received signal samples in the subsequent  $(m+1)$ -th block prior to a new iterative phase estimation. In such a way, the phase offset  $\vartheta$  is progressively brought in the vicinity of 0, whatever the initial value is, and so the estimator is brought to operate in a negligible-bias zone. This is demonstrated in Figure 3, where the phase-precorrection based algorithm achieves satisfactory performance also near  $\pm\pi/4$  and multiples.

Figure 4 depicts the frequency MEV curves of the ISDD algorithm (i.e., the average estimated value  $E\{\hat{\nu}T\}$  as a function of the true frequency normalized offset  $\nu T$ ) for  $M = 12$  decoder iterations,  $E_b/N_0 = 6$  dB and with different length for the FFT size, namely,  $N_{FFT} = 512, 1024, 2048, 4096$ . Applying the estimation procedure based on (15)-(16), it can be noted that  $N_{FFT} = 1024$  is needed to estimate a frequency offset up to  $\nu T = 2 \cdot 10^{-4}$  with a negligible estimation bias.

##### 4.2. RMSEE curves

Performance assessment of the ISDD estimator is concluded with the evaluation of the rms estimation error. Specifically, Fig. 5 shows the curve of the phase RMSEE (i.e.,  $\sqrt{E\{(\hat{\vartheta} - \vartheta)^2\}}$ ) of the ISDD algorithm as a function of  $E_b/N_0$  for various values of the true offset  $\vartheta$ , along with the Modified Cram r-Rao Bound (MCRB) [9].

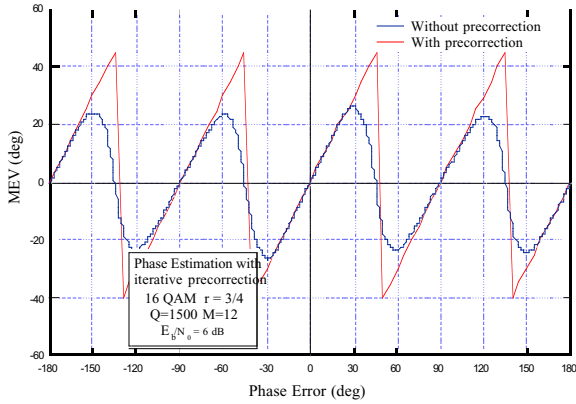


Fig. 3 – Phase Mean Estimated Value (MEV) curves with and without phase pre-correction (ideal frequency recovery).

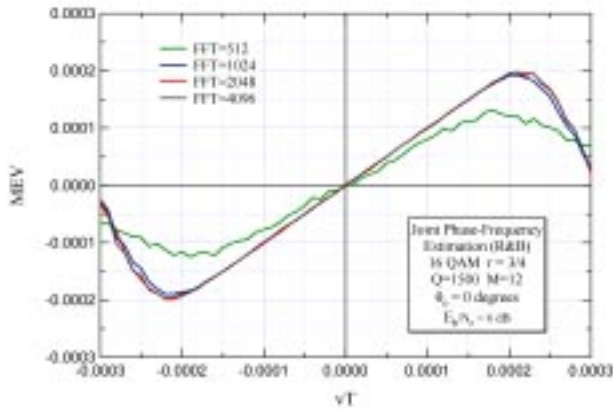


Fig. 4 — Frequency Mean Estimated Value (MEV) curves with different FFT sizes.

Ideal DA estimation lies exactly on the MCRB, while on the other hand the RMSEE performance of ISDD attains the bound only when  $E_b/N_0 \geq 6$  dB, that is when soft data decisions are reliable enough, and thus the performance of the ISDD estimator tends to DA. It is also noted that the RMSEE curve for conventional HDD phase estimation is catastrophic. This is easily explained by noting that the BER of hard-detected 16-QAM in our SNR range is quite poor. This means that hard decisions are not reliable, and so the relevant phase estimate cannot be but inaccurate.

Figure 6 shows the curves of the frequency RMSEE (i.e.,  $\sqrt{E\{(\hat{v}T - vT)^2\}}$ ) of the ISDD algorithm as a function of  $E_b/N_0$  for two values of the true frequency offset, namely  $vT = 0$  and  $vT = 10^{-4}$ , along with the corresponding Modified Cram r-Rao Bound (MCRB) [9]. Again, the MRCB is attained only when  $E_b/N_0 \geq 6$  dB. In addition, a small performance degradation is achieved as regards the estimation of the offset  $vT = 10^{-4}$  with respect  $vT = 0$ . This suggests that the frequency estimation algorithm can be used for frequency tracking, but may

have problems in the acquisition of large (initial) frequency offsets.

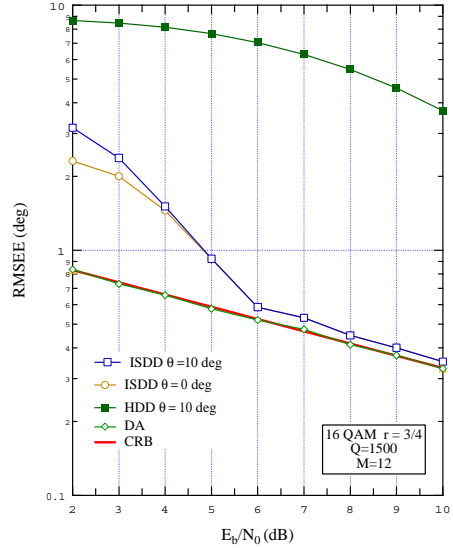


Fig. 5 – Phase Root-Mean Square Estimation Error (RMSEE).

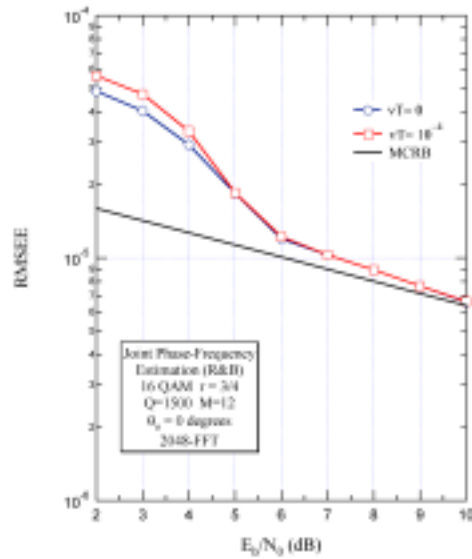


Fig. 6 – Frequency Root-Mean Square Estimation Error (RMSEE).

### 4.3. BER performance

As a summary, Fig. 7 and Fig. 8 show the BER performance in the case of: (i) phase estimation with ideal frequency recovery; (ii) joint phase and frequency estimation. The received signal is demodulated with a turbo decoder equipped with ISDD phase and frequency estimation/correction and with  $M = 10$  decoding iterations. In both charts, the curve for ISDD is compared to the one

with ideal carrier recovery, exhibiting a negligible performance degradation. A significant observation concerns the  $E_b/N_0$  value corresponding to the departure of the RMSEE curves of ISDD from the MCRB. The knee point is in fact located at that SNR value where the BER curve enters the so-called waterfall region, that is, at roughly  $E_b/N_0 = 6\text{dB}$  for 16-QAM, just where the MCRB is attained in Figs. 7 and 8.

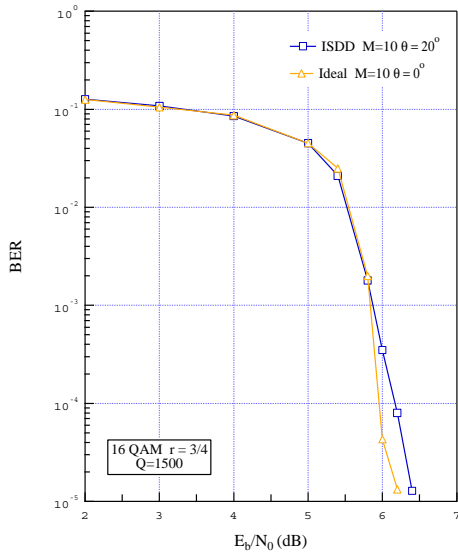


Fig. 7 – BER of turbo-coded 16-QAM with ISDD phase recovery.

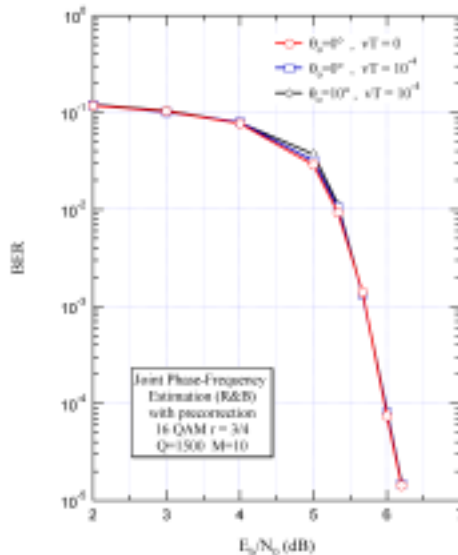


Fig. 8 – BER of turbo-coded 16-QAM with ISDD joint phase and frequency recovery.

## 5. SUMMARY AND CONCLUSIONS

We investigated in this paper a novel soft-decision-directed low-complexity joint phase and frequency estimation algorithm for coherent detection and decoding of a QAM turbo coded signal. Our main findings are: i) for both phase and frequency estimation the estimator bias is negligible, provided that the decoding iterations are at least 10-12; the phase/frequency RMSSE achieves the MRCB when  $E_b/N_0 \geq 6\text{dB}$  (BER waterfall region of the turbo code); the overall BER curves show that iterative carrier estimation combined with iterative decoding has negligible degradation with respect to ideal coherent detection.

## REFERENCES

- [1] C. Berrou, A. Glavieux, Near Optimum Error Correcting Coding and Decoding: Turbo Codes, *IEEE Trans. Comm.*, vol. 44, n. 10, pp. 1261-1271, Oct. 1996.
- [2] The Turbo Principle : From Theory to Practice, *IEEE Journal on Selected Areas on Comm.*, vol. 19, n. 5, May 2001.
- [3] W. E. Ryan, A Turbo Code Tutorial, on <http://www.ece.arizona.edu/~ryan/>, 1998.
- [4] C. Morlet, M.L. Boucheret, I. Buret, Low-Complexity Carrier-Phase Estimator Suited On-Board Implementation, *IEEE Trans. Comm.*, vol. 48, n. 9, pp. 1451-1454, Sept. 2000.
- [5] C. Langlais, M. Helard, Phase Carrier for Turbo Codes over a Satellite Link with the Help of Tentative Decisions, *2<sup>th</sup> International Symposium on Turbo Codes & Related Topics*, vol. 5, n. 4, pp. 439-442, Sept. 2000.
- [6] M. J. Nissila, S. Pasupathy, A. Mammela An EM Approach to Carrier Phase Recovery in AWGN Channel, *IEEE ICC2001*, June 2001.
- [7] A. Anastasopoulos, K. M. Chugg, Adaptive Iterative Detection for Phase Tracking in Turbo-Coded Systems, *IEEE Trans. Comm.*, vol. 49, n. 12, pp. 2135-2144, Dec. 2001.
- [8] G. Colavolpe, G. Ferrari, R. Raheli, Noncoherent Iterative (Turbo) Detection, *IEEE Trans. Comm.*, vol. 48, n. 9, pp. 1488-1498, Sept. 1999.
- [9] U. Mengali, A. N. D Andrea, *Synchronization Techniques for Digital Receivers*, Plenum, New York, 1997.
- [10] V. Lottici, M. Luise, Carrier Phase Recovery for Turbo-Coded Linear Modulations, *IEEE ICC2002*, Apr. 2002.